# Mathematical modelling of radiation-induced cancer risk from breast screening by mammography


## Abstract

**Objectives:** Establish a method to determine and convey lifetime radiation risk from FFDM screening.

**Methods:** Radiation risk from screening mammography was quantified using effective risk (number of radiation-induced cancer cases/million). For effective risk calculations, organ doses and examined breast MGD were used. Screening mammography was simulated by exposing a breast phantom for cranio-caudal and medio-lateral oblique for each breast using 16 FFDM machines. An ATOM phantom loaded with TLD dosimeters was positioned in contact with the breast phantom to simulate the client's body. Effective risk data were analysed using SPSS software to establish a regression model to predict the effective risk of any screening programme. Graphs were generated to extrapolate the effective risk of all screening programmes for a range of commencement ages and time intervals between screens.

**Results:** The most important parameters controlling clients' total effective risk within breast screening are the screening commencement age and number of screens (correlation coefficients were -0.865 and 0.714, respectively). Since the tissue radio-sensitivity reduces with age, the end age of screening does not result in noteworthy effect on total effective risk.

**Conclusions:** The regression model can be used to predict the total effective risk for clients within breast screening but it cannot be used for exact assessment of total effective risk. Graphical representation of risk could be an easy way to represent risk in a fashion which might be helpful to clients and clinicians.



**Keywords:** dosimetry, radiation risk, breast screening

## Introduction

Radiation risk refers to the damage produced by ionising radiation due to energy deposition in tissues. The amount of damage is related to radiation dose, radiation source (e.g. whether it is internal or external), length of time of exposure, which organs are exposed to radiation and the individual's sensitivity which is influenced by age and gender [1]. Adverse health effects as a result of exposure to radiation can be classified into two groups: deterministic which follow high radiation doses and result in direct and predictable tissue damage; stochastic effects which follow low radiation doses and may result in cancer development [2].

There are two opposing risk models to estimate the risk from low radiation doses. The first adopts the linear no-threshold principle. According to this model any dose, no matter how small, can result in cancer. The second model proposes that there is a specific threshold for radiation-induced cancer, and below this threshold the radiation dose can be considered as safe [3]. It has been suggested that the best reasonable risk model to describe the relationship between the exposure to low energy radiation and solid cancers incidence is the linear no-threshold model (LNT) [2, 4].

In 2010, the Health Protection Agency (HPA) reported that medical and dental X-ray procedures constituted 90% of man-made radiation sources to the United Kingdom (UK) population [5]. However, the medical radiation exposure to the United States (US) population increased by 600% from 1980 to 2012 [6]. Accordingly, there is a growing need for healthcare professionals to be more conscious of the risks associated with imaging when using ionising radiation for diagnostic purposes [7]. This is particularly true for mammography breast screening programmes where asymptomatic women are imaged [8]. Also, when screening frequency is increased, because of increased risk of breast cancer [9], radiation risk also increases as a direct consequence of mammography imaging. Extra diligence should therefore be exercised when assigning a woman into a high risk cancer category in which more frequent mammography screening is required. Overall, the radiation risk from screening mammography is considered to be low [10, 11]. Nevertheless, the health profession needs to understand the radiation risks to the woman from mammography imaging, in order to justify serial imaging at any frequency level.

To date, radiation risk has tended to be expressed in terms of dose to the breast (mean glandular dose, MGD) which can be a difficult concept to understand by some imaging staff and referring clinicians. Equally the woman has to make an informed decision about participating in screening taking into account the potential harm the radiation might bring against the benefit of the programme [12].

The work presented here applies previously published data by M.Ali et al. [13] which measured the direct absorbed radiation dose from the examined breast, contralateral breast and 19 other organs across 16 FFDM machines to estimate lifetime effective risk of radiation induced cancer for the UK Breast Screening Programme. Here we develop the model further to establish a

method for estimating & conveying lifetime induced cancer risk from breast cancer screening (from FFDM) for an average woman, with average breast size and density across a lifetime for a range of different FFDM screening scenarios. The method proposed is comprehendible and can be used by referring clinicians and breast screening organisations worldwide in the justification process and during the development of recommendations. Further, women will be able to make an informed decision on whether to attend breast screening.

## Method

To calculate effective risk, organ dose data was required for all four mammography projections along with lifetime attributable risk (LAR) factors for all ages that screening takes place ranging from 25 years, the earliest probable age of screening for high risk clients in the US, to 75 years the latest age of screening end worldwide [13]. Two breast phantoms, attached to an adult dosimetry phantom, were exposed on 16 FFDM machines (Table 1) located in breast screening services within the UK. MGD was calculated; all other organ doses were measured directly using thermoluminescent dosimeters (TLD) as reported previously by M.Ali et al. [13]. LAR factors were calculated for a range of ages using a linear extrapolation method. Dose and LAR data were analysed to generate scenarios in order to calculate total effective lifetime risk values.

### *Phantoms*

To replicate simulated breast thickness and shape in different positions, two breast phantoms constructed of polymethyl methacrylate- polyethylene (PMMA-PE) slabs were used. The Cranio-caudal (CC) phantom was semi-circular of 95mm diameter and 53mm thickness (32.5mm PMMA and 20.5mm PE); the medio-lateral oblique (MLO) was rectangular of 100×150 $mm^2$ area and 58mm thickness (32.5mm PMMA and 25.5mm PE). These breast phantoms simulate an average breast thickness with 29% breast density [14, 15]. According to Yaffe et al. this density can be considered as the common breast density because they found that 95% of 2831 Canadian women have a breast density of less than 45% [16]. 280 calibrated TLD-100H dosimeters (Thermo Scientific, USA) were accommodated inside an adult ATOM dosimetry phantom (CIRS Inc, Norfolk, Virginia, USA) to measure the radiation dose received by 20 different body organs (indicated in Figure 3). Harshaw TLD-100H dosimeters can measure radiation doses across a wide range (1 pGy-10 Gy) with linear response at this energy range (according to the manufacture guidelines [17]. The total uncertainty, due to sensitivity difference and consistency, associated with the detector readings is less than 5%. The ATOM phantom was positioned in contact with the breast phantom to simulate the female body (Figure 1). MGD was calculated using the Institute of Physics and Engineering in Medicine (IPEM) method [18], which is based on the work published by Dance et al. [19].

### *Exposing the phantom*

The breast phantoms (and ATOM phantom) were exposed on 16 FFDM machines (see Table 1); exposures were repeated 3 times on each occasion and then averaged to minimise random error.

Since the full automatic exposure control (including kV, mAs and target/filter combination) is recommend by the European commission [20], full automatic exposure control was used to expose the breast phantoms on each occasion.

*Calculation of lifetime effective risk*

Organ doses together with tissue specific LAR for the US population (BEIR VII phase 2 report) [4] were used to calculate effective risk from 25 to 75 years, using Brenner's equation [21].

$$R=\sum r_T H_T$$

Where R is the effective risk, $r_T$ is the cancer LAR for tissue *T* per unit equivalent dose of that tissue, and $H_T$ is the equivalent dose for tissue *T*. For each organ, the radiation dose was determined by averaging organ dose values from the sixteen FFDM machines. For breast tissue a total of both examined breast MGD and contralateral breast dose were used.

Since LAR factors are published for each decade of life and our method requires the tissue LAR value for each year it was necessary to estimate LAR values for the missing years. A linear relationship between LAR value for each decade of life was used (Figure 2).

*Data analysis*

In order to get good statistical power, two hundred and seventy four different screening scenarios were proposed which comprised of different commencement / end ages (25-75 years) and screening frequencies. For each proposed lifetime interval, such as 25-75 years, 30-75 years, and 30-70 years, we scheduled three different screening categories with regard to screening frequency (annual, biennial, or triennial). Lifetime risk data, arising from the 274 scenarios were analysed in SPSS software (version 22.0, IBM, Armonk, New York, USA) to generate a mathematical regression model and relationship establishment between total effective risk and number of screens and commencement / end ages. The standard error of the estimate was calculated using SPSS software as the square root of the residual mean square to provide a measure of prediction accuracy of the regression model. Spearman's correlation was used to determine the effect of screening commencement age, screening ending age and number of screens on effective lifetime risk. The statistical significance of each correlation was tested using a t-test. To improve accuracy, for each screening frequency (annual, biennial, triennial) a relationship graph between screening commencement age and total effective risk has been obtained considering the screening ending age is constant at 75 years. For each graph 50 different screening scenarios were proposed; the screening commencement age ranged from 25-74 year.

## Results

The total MGD, for both CC and MLO views, for the sixteen considered FFDM machines was 2.019 (1.871-2.166) mGy; mean (95% CI). The minimum recorded MGD was 1.678 mGy, while the maximum MGD was 2.806 mGy. Despite these differences, all values were within the acceptable range recommended by national mammographic protocols [20].

For organs other than the examined breast, it was found that for some organs the radiation dose was zero. This means that either these organs did not receive radiation dose during screening mammography exposure or the dose received by these organs was below the sensitivity threshold of the TLDs. However, some organs received radiation dose ranging from less than 1μGy to more than 25 μGy (Figure 3). The contralateral breast tissue received the second highest radiation dose after the examined breast; 28.75 [24.20 - 33.3] μGy (mean [95% CI]). However, sternum bone marrow radiation dose was the highest bone marrow dose and the third highest organ dose after the examined and contralateral breasts; 19.07 [15.81 - 22.34] μGy (mean [95% CI]).

For each year of female lifetime the mean effective lifetime risk from one screening visit, along with the 95% confidence interval (CI) for the 16 FFDM machines is included in Table 2. The effective lifetime risk is shown to decrease with age.

The effect of screening commencement age, number of screens and ending age of screening on the total effective risk was evaluated using Spearman's correlation coefficient (Table 3). There is strong correlation between the total effective risk and both screening commencement age and number of screens during female lifetime.

Using SPSS, a backward stepwise regression model was generated to predict the total effective risk of any screening programme with regard to commencement / end ages of screening and number of screens. The regression model is summarised in Table 4. The regression equation elucidates the effect magnitude of each parameter on effective lifetime risk. The validity of any regression model is determined by its ability to assess the outcome (total effective risk) variability by predictors' variability (adjusted $R^2$), and the interval of predicted outcome (variation coefficient).

If screening mammography ending age is set at a constant level (75 years old), the factors that affect the total effective risk reduced down to only two (commencement age and screening frequency). The resultant graphical relationship between screening commencement age (year) on the X-axis and average total effective risk (case/$10^6$) for the sixteen FFDM machines on the Y-axis is demonstrated in Figure 4 which contains three relationship lines; one for each screening frequency (annual, biennial, and triennial).

## Discussion

Several researchers have assessed the radiation dose to other body tissues and organs from mammography; here *other* refers to all organs with the exclusion of the examined breast. In all instances, their approaches were different to the methods used here. For instance, Sechopoulos, Suryanarayanan , Vedantham , D'Orsi, and Karellas [22] used Monte Carlo dose simulation, while Hatziioannou et al. [23] used TLDs accommodated inside Lucite phantom to measure radiation dose received by several organs during cranio-caudal and medio-lateral breast exposures. Organ radiation doses measured in this work showed some differences between the sixteen FFDM machines (Figure 3). For instance, for some FFDM machines the third highest other organ radiation dose was received by clavicular bone marrow (after contralateral breast and sternum bone marrow), while for other machines the thyroid radiation dose ranks as the third highest dose. However, these organ dose differences do not result in large variations in calculated total effective lifetime risk because examined breast MGD results in up to 98% of effective lifetime risk and other organs cause only 2%.

Statistical analysis illustrates that there is a strong correlation between total effective risk and both screening commencement age and number of screens. The correlation coefficients were -0.865 and 0.714, respectively. This means that the total effective risk increases with early screening commencement age and a greater number of screens. However, a weak correlation is seen between the total effective risk and the end age of screening (-0.346). This suggests that for any screening programme the total effective risk decreases with increased end age of screening.

The regression model can be used to predict the total effective risk for any screening programme by the screening commencement age, number of screens and ending age of screening. However, any regression model has an associated error. Our regression model can explain 87% of total effective risk variability by other parameter variability (adjusted $R^2 = 0.87$). For prediction purposes, the predicted total effective risk intervals are wide, with a coefficient of variation for the model around 31%. The addition of time interval between screens as a predictor to the regression model does not increase the model's accuracy; its effect is statistically non-significant.

For accurate calculation of total effective risk for any screening programme we established a relationship graph (Figure 4). To generate the graph, effective risk data for ages 25-75 years were used to propose different screening scenarios with regards to the screening commencement age and time interval between screens, these were the most important factors affecting the radiation effective risk. The proposed commencement ages ranged from 25 years, the earliest probable age of screening mammography for high risk women, to 74 years. One, two, and three year time intervals were considered in our scenarios. Since human tissue radio-sensitivity reduces greatly after age of 70 years and most worldwide screening programmes end between the ages 70-75 years [24], the ending age of screening mammography does not generate large differences in calculated total effective lifetime risk. Accordingly, the ending age of screening

mammography was considered as 75 years in all of our scenarios. The graph comprises of three lines, one for each time interval, so it can be easily used to evaluate the total effective risk of any screening programme by the commencement age of screening using interpolation method.

The main advantage of our graphical data is that they represent an easy way for radiation risk estimation from screening mammography to be illustrated. The graph can be simply used by clinicians/referrers or practitioners, and the graphical data are more likely to be understandable by the women than MGD. It is useful for screening mammography justification in terms of harms versus benefits especially for high breast cancer risk women who are invited for early and more frequent screening mammography than average breast cancer risk women. Moreover, the radiation risk to other body tissues and organs are included in this model.

The major limitation of our model is that it was generated for an average size woman who has an average breast thickness and density. Accordingly our data are applicable for a breast with 29% density and 53 mm CC thickness. Thicker and more dense breasts require higher exposure factors (kV and mAs) resulting in higher MGD and consequently more risk of radiation-induced breast cancer. This limitation can be addressed by future work using different size body phantoms with a series of breast phantoms simulating a range of breast thicknesses and densities. Since FFDM is the only available technique for screening in the UK, this model was designed to assess the radiation risk when FFDM used. However, other mammographic modalities (computed radiography and film screen mammography) were not considered. Finally, the LAR factors used in the model generation were for Euro-American population. Accordingly, further work is required for other populations.

A further limitation of our model is that it does not take into account genetic factors which increase the risk of developing breast cancer. Clinically, of these breast cancer susceptibility genes, BRCA1 and BRAC2 are most important. The risk of developing breast cancer among mutation carriers of these genes by the age of 70 is 65% and 45% respectively [25]. In order to address this issue, we are preparing a study on the impact of these and other genetic factors. Adding these factors to our statistical model as a covariate may lead to a refinement of our model and ultimately to a more accurate estimation of the true impact of mammography screening on the total effective risk.

Overall our method can be used to establish a mathematical model for radiation risk assessment from any screening procedure involving ionising radiation such as breast cancer screening using digital breast tomosynthesis or dedicated breast computed tomography. The incorporation of breast density, breast size, genetic factors and different screening procedures (involving ionising radiation) into the model would enable the estimation of risk to be personalised for individual screening clients. This is the subject of our future work.

## Conclusion

The multiple linear regression models can be considered useful for the prediction of the radiation-induced cancer from screening programmes for an average woman, albeit with a variation of 31%. Graphical representation of data, based upon scenarios, will have a value for informing clinicians/referrers and screening clients about the radiation risks from FFDM screening as the information is presented in a form which is easily understood compared with MGD.

## References


1. Health Protection Agency (HPA), *Risk of solid cancers following radiation Exposure: estimates for the UK population*. 2011, Health Protection Agency: Oxfordshire.
2. Intennational Commission on Radiological Protection (ICRP), *The 2007 Recommendations of the International Commission on Radiological Protection. ICRP publication 103.* Ann ICRP, 2007. **37**(2-4): p. 1-332.
3. Prasad, K.N., W.C. Cole, and G.M. Hasse, *Health risks of low dose ionizing radiation in humans: a review.* Exp Biol Med (Maywood), 2004. **229**(5): p. 378-82.
4. National Academy of Sciences (NAS), *Health Risks from Exposure to Low Levels of Ionizing Radiation: BEIR VII – Phase 2*. 2006, National Academies Press: Washington.
5. Hart, D., et al., *Frequency and collective dose for medical and dental x-ray examinations in the UK, 2008*. 2010.
6. Linet, M.S., et al., *Cancer risks associated with external radiation from diagnostic imaging procedures.* CA Cancer J Clin, 2012. **62**(2): p. 75-100.
7. Benevides , L.A., et al., *Dosimetry in Mammography: Average Glandular Dose Based on Homogeneous Phantom.* 2011: p. 231-248.
8. Bosmans, H. and N. Marshall, *Radiation Doses and Risks Associated with Mammographic Screening.* Current Radiology Reports, 2013. **1**(1): p. 30-38.
9. Yaffe, M.J. and J.G. Mainprize, *Risk of radiation-induced breast cancer from mammographic screening.* Radiology, 2011. **258**(1): p. 98-105.
10. Myronakis, M.E., M. Zvelebil, and D.G. Darambara, *Normalized mean glandular dose computation from mammography using GATE: a validation study.* Phys Med Biol, 2013. **58**(7): p. 2247-65.
11. Marmot, M.G., et al., *The benefits and harms of breast cancer screening: an independent review: A report jointly commissioned by Cancer Research UK and the Department of Health (England) October 2012.* British Journal of Cancer, 2013. **108**(11): p. 2205-2240.
12. Michell, M.J., *Breast screening review--a radiologist's perspective.* Br J Radiol, 2012. **85**(1015): p. 845-7.
13. M. Ali, R., et al., *A method for calculating effective lifetime risk of radiation-induced cancer from screening mammography.* Radiography, 2015. **21**(4): p. 298-303.
14. Feng , S.S., B. Patel, and I. Sechopoulos, *Objective models of compressed breast shapes undergoing mammography.* Med Phys, 2013. **40**(3): p. 031902.
15. Bouwman, R.W., et al., *Phantoms for quality control procedures in digital breast tomosynthesis: dose assessment.* Phys Med Biol, 2013. **58**(13): p. 4423-38.
16. Yaffe , M.J., et al., *The myth of the 50-50 breast.* Medical Physics, 2009. **36**(12): p. 5437.
17. ThermoScientific. *High Sensitivity LIF: Mg, Cu, P Thermoluminescent Dosimetry Materials, Chips*. 2015 [cited 2016 07-28]; Available from:

https://www.thermofisher.com/order/catalog/product/SCP18815#%2Flegacy=thermoscientific.com.
18. Institute of Physics and engineering in Medicine (IPEM), *The commissioning and routine testing of mammographic X-ray systems*. 2005, IPEM: York.
19. Dance, D.R., et al., *Additional factors for the estimation of mean glandular breast dose using the UK mammography dosimetry protocol.* Physics in medicine and biology, 2000. **45**: p. 3225–3240.
20. European Commission, European guidline for quality assurance in breast cancer screening and diagnosis : fourth edition supplements. 2013: Belgium.
21. Brenner, D.J., *We can do better than effective dose for estimating or comparing low-dose radiation risks.* Ann ICRP, 2012. **41**(3-4): p. 124-8.
22. Sechopoulos , I., et al., *Radiation dose to organs and tissues from mammography: Monte Carlo and phantom study.* Radiology, 2008. **246**(2): p. 434-443.
23. Hatziioannou, K.A., et al., *Dosimetric considerations in mammography.* Eur. Radiol., 2000. **10**(7): p. 1193-1196.
24. International Cancer Screening Network (ICSN), *Breast Cancer Screening Programs in 26 ICSN Countries, 2012: Organization, Policies, and Program Reach*. 2015 [cited 2015; Available from: http://healthcaredelivery.cancer.gov/icsn/breast/screening.html.
25. Antoniou, A., et al., Average risks of breast and ovarian cancer associated with BRCA1 or BRCA2 mutations detected in case Series unselected for family history: a combined analysis of 22 studies. Am J Hum Genet, 2003. 72(5): p. 1117-30.

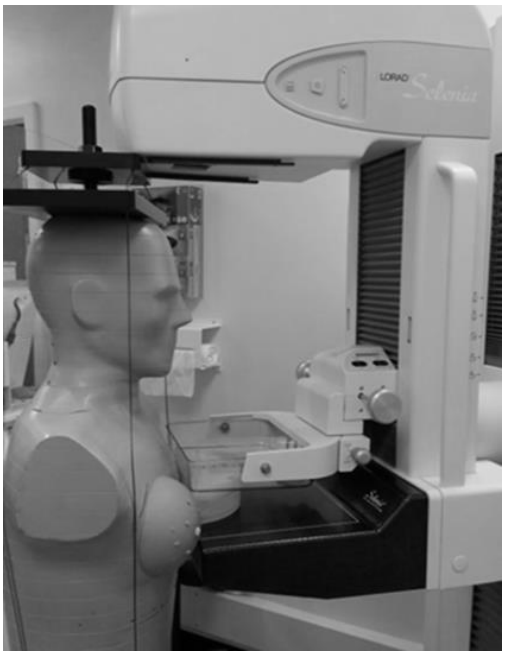



**(1a)** **(1b)**

**Figure (1)** Breast and ATOM phantoms positioned on FFDM machine **(a)** in cranio-caudal position **(b)** in medio-lateral oblique position.

**Table (1)** Study FFDM machines.

| Machine Brand | Target/filter combination | Number of machines |
|---|---|---|
| Hologic Selenia | Mo/Mo | 1 |
| Hologic Selenia | Rh/Rh | 2 |
| Hologic Selenia Dimensions | W/Rh | 2 |
| GE Seno Essential | Rh/Rh | 8 |
| Giotto | W/Ag | 1 |
| Siemens Mammomat Inspiration | W/Rh | 2 |
| Total | 16 | |

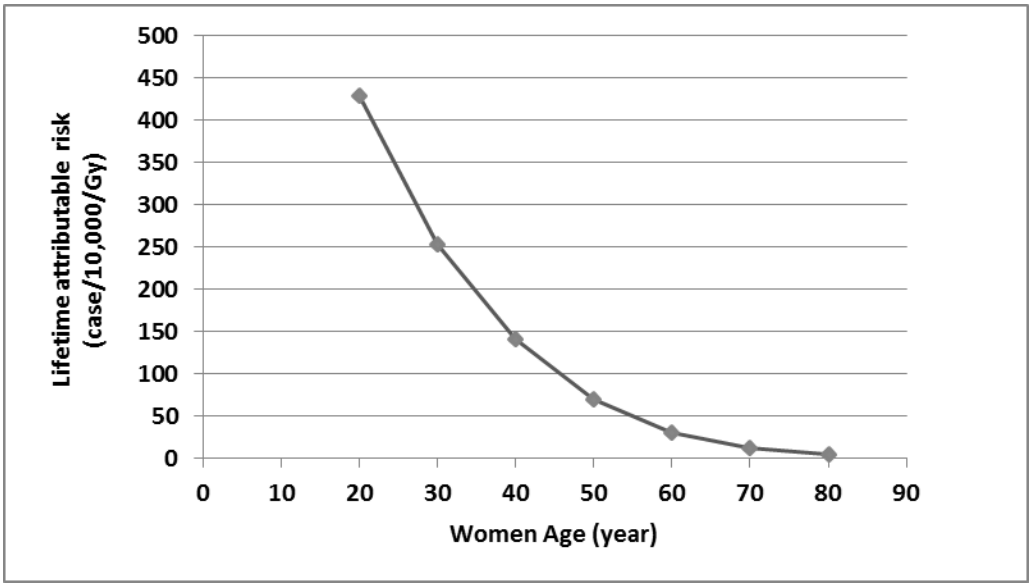


**Figure (2)** Breast tissue LAR extrapolation using linear relationship between each decade LAR values.

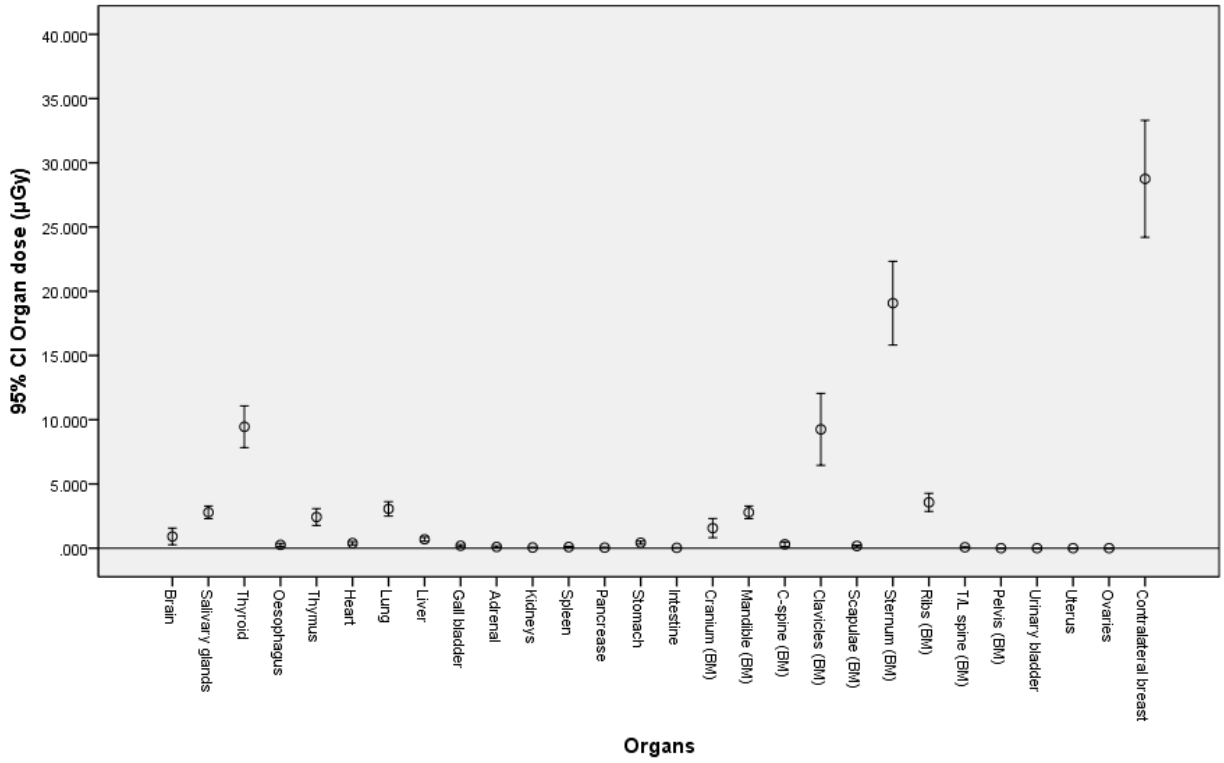


**Figure (3)** The mean organ doses across the sixteen FFDM machines (circles) with 95% CI (error bars) for one screening visit (CC and MLO projections for each breast) as measured using TLDs.

**Table (2)** Mean calculated effective lifetime risk values for each year of female life with 95% CI. The 95% CI reflects variation in absorbed dose from the 16 FFDM machines.

| Age (year) | Effective lifetime risk (case/$10^6$) | | Age (year) | Effective lifetime risk (case/$10^6$) | |
|---|---|---|---|---|---|
| | Mean | 95% CI | | Mean | 95% CI |
| 25 | 70.0 | [64.9 - 75.1] | 51 | 13.6 | [12.6 - 14.6] |
| 26 | 66.4 | [61.5 - 71.2] | 52 | 12.8 | [11.9 - 13.8] |
| 27 | 62.8 | [58.2 - 67.4] | 53 | 12.0 | [11.1 - 12.9] |
| 28 | 59.2 | [54.8 - 63.5] | 54 | 11.2 | [10.4 - 12.0] |
| 29 | 55.5 | [51.5 - 59.6] | 55 | 10.4 | [9.7 - 11.2] |
| 30 | 51.9 | [48.1 - 55.7] | 56 | 9.6 | [8.9 - 10.3] |
| 31 | 49.6 | [46.0 - 53.3] | 57 | 8.8 | [8.2 - 9.5] |
| 32 | 47.3 | [43.9 - 50.8] | 58 | 8.0 | [7.4 - 8.6] |
| 33 | 45.0 | [41.8 - 48.3] | 59 | 7.2 | [6.7 - 7.8] |
| 34 | 42.7 | [39.6 - 45.9] | 60 | 6.4 | [6.0 - 6.9] |
| 35 | 40.5 | [37.5 - 43.4] | 61 | 6.0 | [5.6 - 6.5] |
| 36 | 38.2 | [35.4 - 41.0] | 62 | 5.6 | [5.2 - 6.1] |
| 37 | 35.9 | [33.2 - 38.5] | 63 | 5.3 | [4.9 - 5.6] |
| 38 | 33.6 | [31.1 - 36.0] | 64 | 4.9 | [4.5 - 5.2] |
| 39 | 31.3 | [29.0 - 33.6] | 65 | 4.5 | [4.1 - 4.8] |
| 40 | 29.0 | [26.9 - 31.1] | 66 | 4.0 | [3.8 - 4.4] |
| 41 | 27.5 | [25.5 - 29.5] | 67 | 3.7 | [3.4 - 4.0] |
| 42 | 26.1 | [24.2- 28.0] | 68 | 3.3 | [3.1 - 3.5] |
| 43 | 24.6 | [22.8 - 26.4] | 69 | 2.9 | [2.7 - 3.1] |
| 44 | 23.2 | [21.5 - 24.8] | 70 | 2.5 | [2.3 - 2.7] |
| 45 | 21.7 | [20.1 - 23.3] | 71 | 2.3 | [2.2 - 2.5] |
| 46 | 20.2 | [18.8 - 21.7] | 72 | 2.2 | [2.0 - 2.3] |
| 47 | 18.8 | [17.4 - 20.2] | 73 | 2.0 | [1.9 - 2.2] |
| 48 | 17.3 | [16.1 - 18.6] | 74 | 1.8 | [1.7 - 2.0] |
| 49 | 15.9 | [14.7 - 17.0] | 75 | 1.7 | [1.6 - 1.8] |
| 50 | 14.4 | [13.4 - 15.5] | | | |

CI, confidence intervals. Effective lifetime risk refers to an individual's chance of acquiring a radiation-induced cancer.

**Table (3)** The association of different parameters with effective lifetime risk determined by Spearman's correlation coefficient. Statistical significance was tested using t-test.

| Commencement age | Ending age | Number of screens |
|---|---|---|
| -0.865 | -0.346 | 0.714 |
| All values were statistically significant (P<0.001). | | |

**Table (4)** Multiple linear regression equation. The standard error of the estimate was calculated in SPSS as the square root of the residual mean square.

| Regression Equation | Adjusted $R^2$ | Std. Error of Estimate | Variation Coefficient |
|---|---|---|---|
| TR= 705.170 –7.763 C – 6.085 E + 17.569 N | 0.870 | 91.127 | 0.312 |
| TR, total effective lifetime risk; N, number of screens; C, commencement age of screening; E, ending age of screening. | | | |

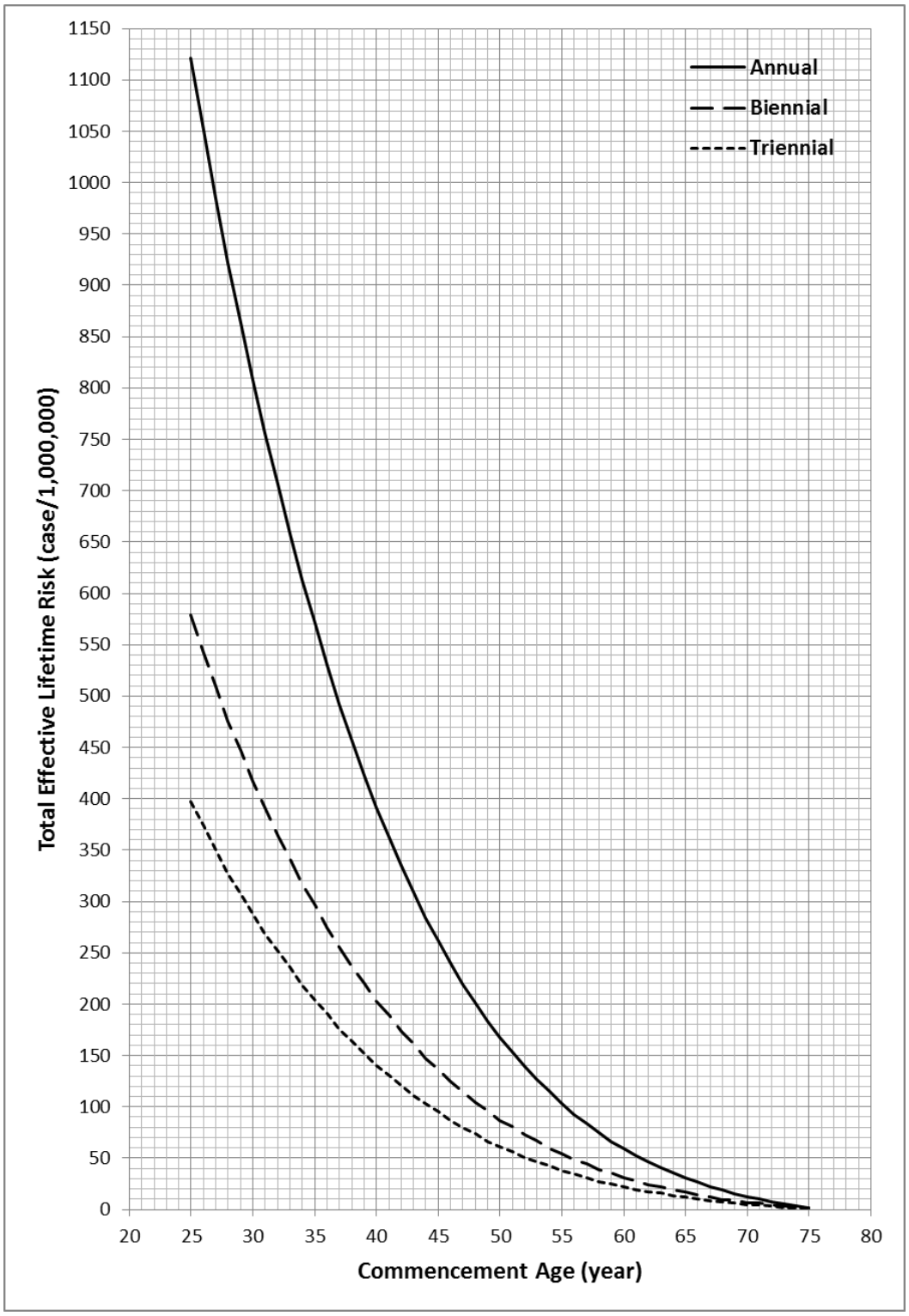


**Figure (4)** Total effective lifetime risk of screening mammography ending at age of 75 years (data based on calculated total effective risk of 50 scenarios of different commencement age for each screening frequency)